Seventh Framework Programme
Theme 9 Space FP7-SPA.2009.1.1.02
Monitoring of climate change issues (extending core service activities)

Grant agreement for: Collaborative Project (generic).
Project acronym: **MONARCH-A**
Project title: **MONitoring and Assessing Regional Climate change in High latitudes and the Arctic**
Grant agreement no. 242446
Start date of project: 01.03.10
Duration: 36 months
Project coordinator: Nansen Environmental and Remote Sensing Center, Bergen, Norway

D2.5.1: Improved estimate of the ocean circulation and sea level with at least 1/6 ° spatial resolution.

D2.5.2 - Improve ECVs over the Arctic Ocean, including sea ice cover, sea ice transports, sea level and ocean transports of heat and freshwater.

Due date of deliverable: 25.05.2013

Actual submission date: 25.05.2013

Organization name of lead contractor for this deliverable: UHAM

Project co-funded by the European Commission within the Seventh Framework Programme, Theme 6 Environment		
Dissemination Level		
PU	Public	X
PP	Restricted to other programme participants (including the Commission)	
RE	Restricted to a group specified by the consortium (including the Commission)	
CO	Confidential, only for members of the consortium (including the Commission)	

ISSUE	DATE	CHANGE RECORDS	AUTHOR
0	08/04/2011	Template	K. Lygre
1	25/05/2013	1st version	N. Koldunov
2	28/04/2013	Minor editing on the lay-out	K. Lygre

SUMMARY

A description is being provided of a data assimilation system used to obtain improved estimate of the ocean circulation and sea level. The system is based on the Massachusetts Institute of Technology General Circulation Mode (MITgcm). The model setup covers the Arctic between 50N in the Atlantic and the Bering strait. The system consists of a coupled ocean-ice adjoint model set up for sea ice assimilation.

The adjoint assimilation technique allows us to obtain dynamically consistent model solution that was brought into consistency with observations while obeying model dynamics. As a result of assimilation the overall decrease in the data-model differences is considerable but is different for different variables. The largest improvement observed for the sea ice concentration, that on average reach 31%t reduction. The smallest decrease is for the SSH. We briefly analyze spatial distribution of several fields and show how they improve after data assimilation. Also integral vertical distributions of temperature and salinity in different areas of the Arctic Ocean are shown to be improved as well. Results of the model simulations will be distributed through ICDC.

MONARCH-A CONSORTIUM

Participant no.	Participant organisation name	Short name	Country
1 (Coordinator)	Nansen Environmental and Remote Sensing Center	NERSC	NO
2	The University of Sheffield	USFD	UK
3	Universität Hamburg	UHAM	DE
4	Centre National de la Recherche Scientifique	CNRS	FR
5	Scientific foundation Nansen International Environmental and Remote Sensing Center	NIERSC	RU
6	Universitetet i Bergen	UiB	NO
7	Danmarks Tekniske Universitet	DTU	DK
8	Institut Francais de Recherche pour l'Exploitation de la Mer	IFREMER	FR

Table of Contents

List of Figures

List of Tables

1 Introduction

Despite recent increase in amount of observations, the Arctic Ocean continues to be one of the least explored areas of the World Ocean due to harshness of its environmental conditions. Satellite observations of some of the ocean characteristics such as SSH, SST, ocean color and SSS, that are routinely obtained for the rest of the ocean, have strong limitations in the polar regions, due to presence of the sea ice cover, and parameters of the satellite's orbits . Hence in order to understand large scale processes in the Arctic Ocean we have to heavily rely on the numerical ocean models.

Representation of the Arctic Ocean in the ocean models considerably improved during the last 10 years. As part of the MONARCH-A project we compare several state of the art models against observational data generated ether by groups working in the MONARCH-A or obtained from other sources D2.4.1. Our conclusion was, that many models reasonably well reproduce variability of SSH, temperature, salinity, sea ice and currents. The existing level of resemblance between models and available observations allows us to use model data to draw realistic conclusions about variability of the Arctic Ocean parameters, at least on decadal scale, and reveal some of the mechanisms that drive changes in ocean characteristics.

One of the ways to further improve the representation of the Arctic Ocean in circulation models is to use data assimilation techniques. The present rate of changes in the Arctic and the importance of this region for the entire climate system attracted a lot of attention to this problem. Data assimilation is based on the belief that dynamically consistent "interpolation" of oceanographic observations can lead to a better understanding of the mechanisms responsible for observed changes, and, as a side effect, improve atmospheric forcing fields. Moreover reliable decadal predictions are possible only with good initial conditions, and this is what data assimilation can provide.

Within the framework of MONARCH-A we created an assimilation system for the Arctic Ocean, and performed assimilation experiments with medium resolution model for the first decade of the 21st century. This period characterized by significant changes in the Arctic Ocean, and, likely enough, by increased amount of observations. This makes it a good test ground for assimilation system, and promise valuable scientific outcome.

In the following we describe model domain (bathymetry, grid), main characteristics of the model and data assimilation procedure. In the second part of this document we discuss results of assimilation.

2 Model domain and grid

The model domain covers north of the North Atlantic and the Arctic Ocean. The bathymetry is obtained by interpolation of ETOPO2 (two-minute gridded global relief for both ocean and land areas) to the model grid. There is no artificial deepening of or widening of the Nordic Seas passages was applied, so they maintain their true depths and their cross-section areas.

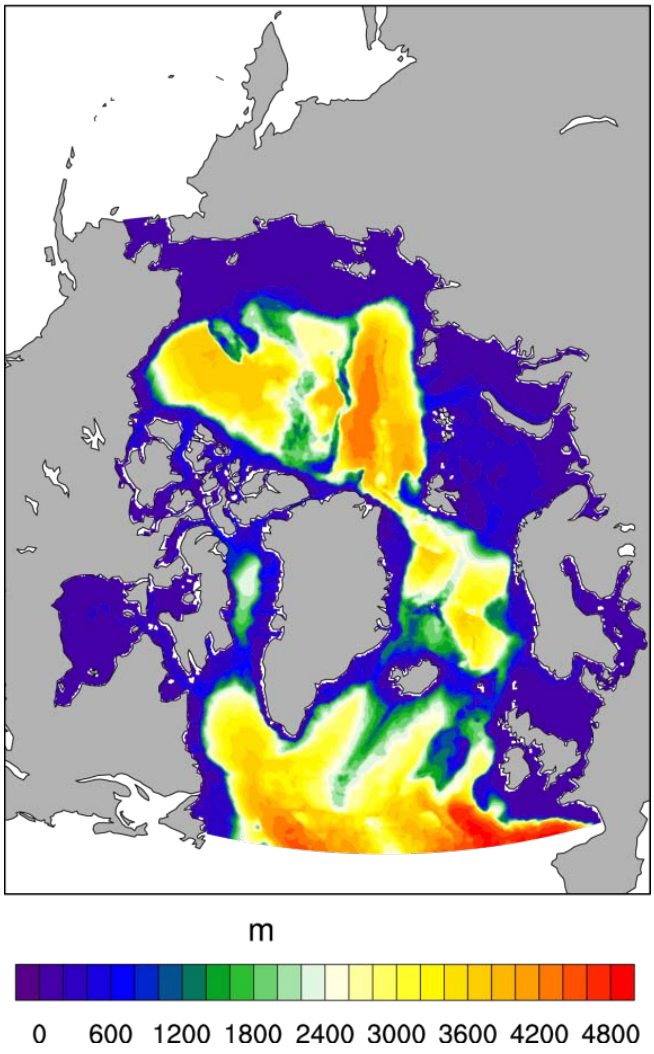

Fig.1 Model domain and bathymetry.

The model grid is curvilinear and is a subset of the ATL06 model grid. It has about 1/6 of a degree spatial resolution that translates in the Arctic Ocean to 15 km horizontal resolution. The original grid is bipolar (one pole over North America and another over the Europe). This solves the problem of the North Pole singularity in the traditional geographical latitude-longitude coordinate system, when meridians converge at the North Pole. Consequently in this configuration there is no severe restrictions on the length of the time step allowed for computational stability of finite difference schemes (Madec et al, 1996). The model use z-coordinates and has 50 levels with resolution vary from 10 meters in the top layers of the water column to 550 meters in the deeper parts of the ocean.

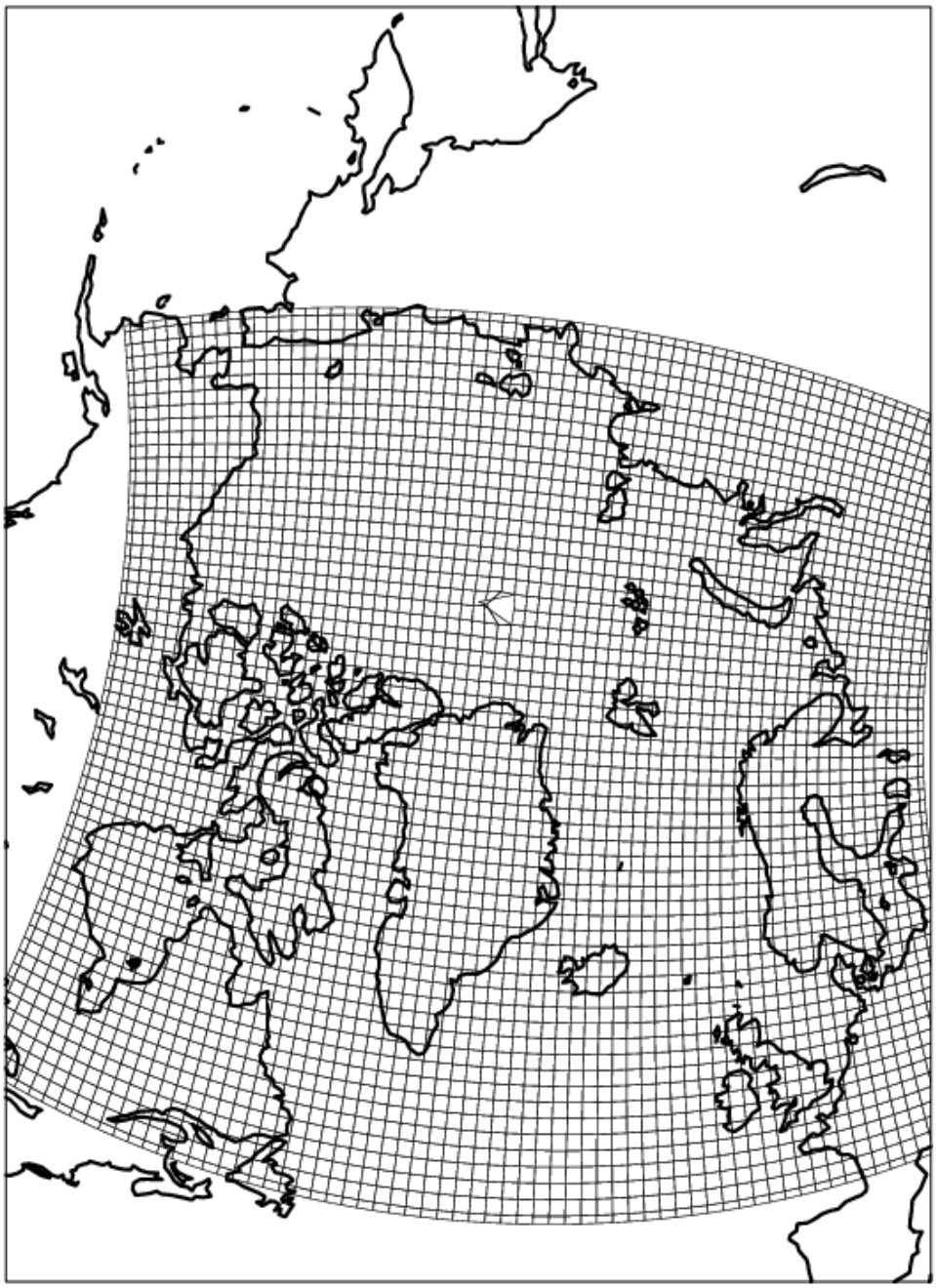

Fig.2 Model grid. Only every 7th grid point is shown for visual convenience.

3 Experimental Setup

As atmospheric forcing the model system use 6 hourly NCEP R1 reanalysis (Kalnay et al., 1996). The following fields are used:

- Mean Daily Air temperature at 2 meter
- Precipitation Rate at surface
- Specific humidity at 2 meter
- Downward Shortwave Radiation Flux
- Net shortwave radiation
- Downward Longwave Radiation Flux
- U-wind at 10 m
- V-wind at 10 m

On the open southern boundary the results from 60-year long solution of ATL06 model are used. The ATL06 in turn is forced by a 1◦ resolution global solution of the MITgcm forced by the same NCEP data set. At the northern boundary a barotropic net inflow of 0.9 Sv into the Arctic is prescribed at Bering Strait, which balances a corresponding outflow through the southern boundary. 2000). An annual averaged river run-off (Fekete et al., 1999) is applied in the North Atlantic, while seasonally varying run-off is used for the Arctic rivers.

The ocean component of the MITgcm model consists of conservation equations for horizontal and vertical momentum, volume, heat, and salt as well as an equation of state. A detailed description of the model is provided by Adcroft et al 2010. The MITgcm offer wide variety of modules that can simulate different aspects of ocean physics. For the vertical mixing parametrization we use the K-Profile Paremeterization (KPP) scheme of Large et al. (1994). Harmonic diffusion along neutral surfaces according to Redi (1982) in association with the parameterization of Gent and Mc Williams (1990) for eddy-induced tracer advection represents unresolved eddy processes. The model is operated in the hydrostatic configuration with an implicit free surface.

The sea ice component is based on the Hibler type (Hibler 1979, Hibler 1980) viscous-plastic dynamic-thermodynamic sea ice model. The thermodynamical part of the model is the so-called zero-layer formulation following the Appendix in (Semtner 1976) with snow cover as in (Zhang et al 1998). The temperature profile in the ice is assumed to be linear with constant ice conductivity. Such a formulation implies that the sea ice does not store heat, and, as a result, the seasonal variability of sea ice is exaggerated (Semtner 1984). To reduce this effect we use the sub-grid scale heat flux parametrization following (Hibler 1984). Moreover, we use the viscous-plastic rheology scheme of

Hibler (1979) with an extended line successive over-relaxation (LSOR) method (Zhang et al 1997). A comparison of the effect of different rheology schemes in MITgcm is provided by Losch et al (2009). Recently Nguyen et al (2011) apply the coupled MITgcm for a regional Arctic Ocean study.

4 Adjoint data assimilation

One of the key features of the MITgcm is its suitability for the automatic generation of its tangent linear and adjoint code, which permits to perform sensitivity and optimization studies. The code for the tangent linear and adjoint models is automatically generated by the Transformation of Algorithms in FORTRAN (TAF) source-to-source translator (Giering and Kaminski 1998; Giering et al 2005). The description of the MITgcm adjoint construction together with its first application for the sensitivity studies has been published by Marotzke et al (1999); examples of subsequent applications of the model during ocean state and parameter estimation studies are provided by Stammer et al (2002); Stammer (2005); Stammer et al (2007); Köhl and Stammer (2008) and by Köhl and Stammer (2004); Stammer et al (2008) for sensitivity studies. Here we use a version of the MITgcm with improved adjoint of a thermodynamic ice model, that was recently developed and applied for ocean-ice state estimates in the Labrador Sea (Fenty and Heimbach 2012a,b).

The process of data assimilation using an adjoint model is iterative. First the forward model run has to be performed to calculate the model data misfit formulated as a cost function. Then the adjoint run is performed to calculate the gradients of this cost function. By using an adjoint coupled sea ice ocean model, one can calculate how sensitive a cost function that depends on the state variable of the model, J (e.g. model-data misfit (as in our case) or mean monthly sea ice area over some region) is to a parameter of the model x (e.g. initial conditions, forcing fields). In essence, the adjoint method allows us to obtain the gradient (or sensitivity) (a) as

$$a = \partial J/\partial x \qquad (1)$$

for every grid point and every time step in such a way that we can estimate the impact of any (sufficiently small) perturbation in x on J simply by multiplying the perturbation in the parameter by the gradient given in eq. 1.

The elegance of the adjoint method is that gradients can be calculated with respect to any number of input variables without extra effort, which, compared to classical sensitivity analysis, makes the approach very efficient in terms of computer time. The remarkable feature of adjoint sensitivities is their ability to reveal non-local influences from remote places or distant times and their path of influence.

The adjoint model was modified here similarly to Köhl and Stammer (2008). Additionally sea ice dynamics were switched off in the adjoint model. The cost function was defined similarly to Köhl et al. (2007), however list of constrains (assimilated variables) is different. Complete list of parameters assimilated and their sources are presented in the Table 1.

Table 1. Data used for assimilation.

Variable	Source
Monthly PHC climatology	**PHC 3.0, Steele et al (2001)** http://psc.apl.washington.edu/nonwp_projects/PHC/Climatology.html
Mean Dynamic Topography	Produced in the framework of the MONARC-A project by DTU.
Monthly SST	Remote Sensing Systems http://www.remss.com/
Sea Level Anomalies from TOPEX/Poseidon, ERS-1,2 and Envisat	AVISO http://www.aviso.oceanobs.com/index.php?id=1270
EN3 hydrographic data	**Curry (2001)** http://www.metoffice.gov.uk/hadobs/en3/
NISE hydrographic data	**Nilsen et al (2008)**
Sea ice concentration	**Cavalieri et al (1996) (NASA Team algorithm)** http://nsidc.org/data/nsidc-0051.html

To bring the model into agreement with observations, we use gradients obtained after the adjoint run and estimate changes that is necessary to apply to so called “control variables”. The control variables are:

- Surface (2-m) air temperature
- Surface (2m) specific humidity
- Surface (10-m) zonal and meridional wind velocity
- Precipitation
- Downward shortwave and longwave radiation
- Initial temperature and salinity (only for the first year of assimilation)

Next forward run of the model use corrections calculated in the previous iteration and data-model misfit calculated again. This process is repeated until changes in the cost function from iteration to iteration decrease by less than 1%.

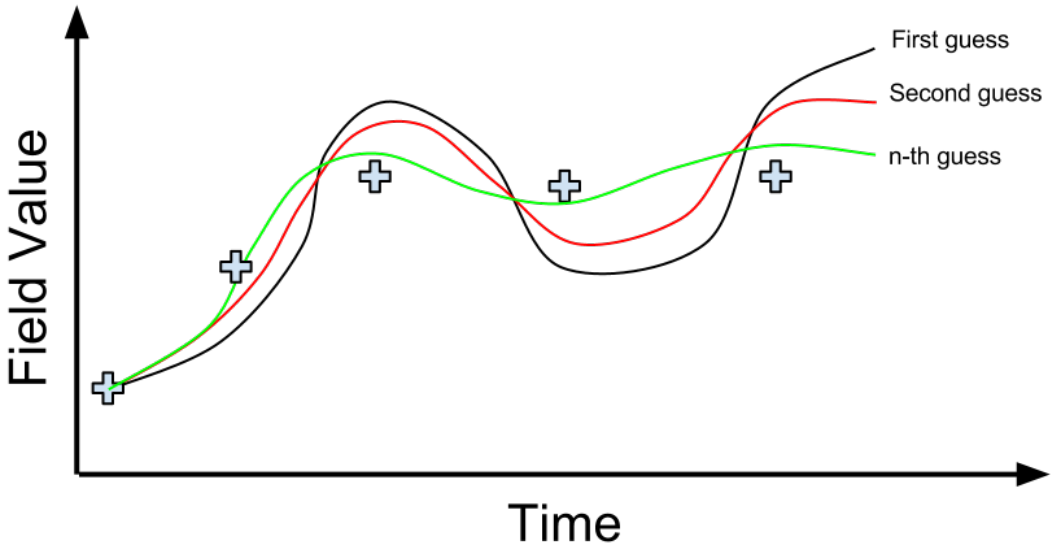

Fig. 3. Schematic representation of iterative process of adjoint data assimilation. Crosses represent observations.

We perform data assimilation by 1 year chunks. After cost function for the year is not getting smaller by value larger than 1% of initial cost function we begin assimilation for the next year. Results of the last successful iteration from the previous year become initial conditions for the next year.

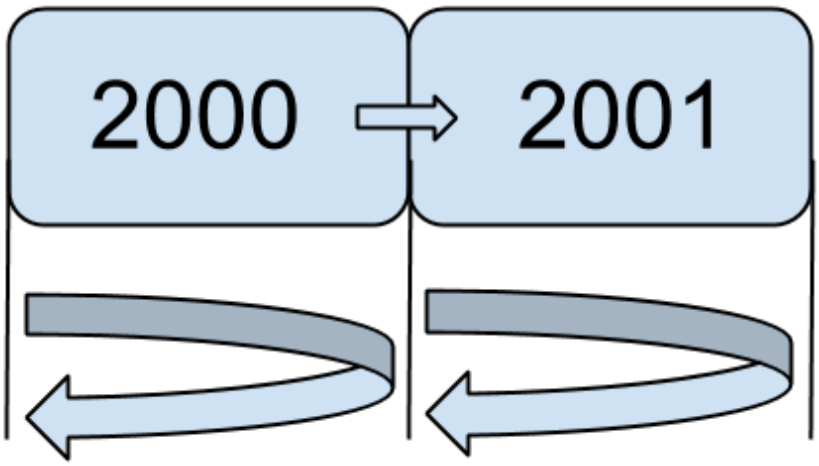

Fig. 4. Schematic representation of 1 year chunks data assimilation experiments.

5 Results

Fig. 5 shows percentage of decrease in model data difference. The red color indicates reduction in total model-data difference (FC), and other show reduction for individual variables. Negative values mean that there is an increase in model-data difference.

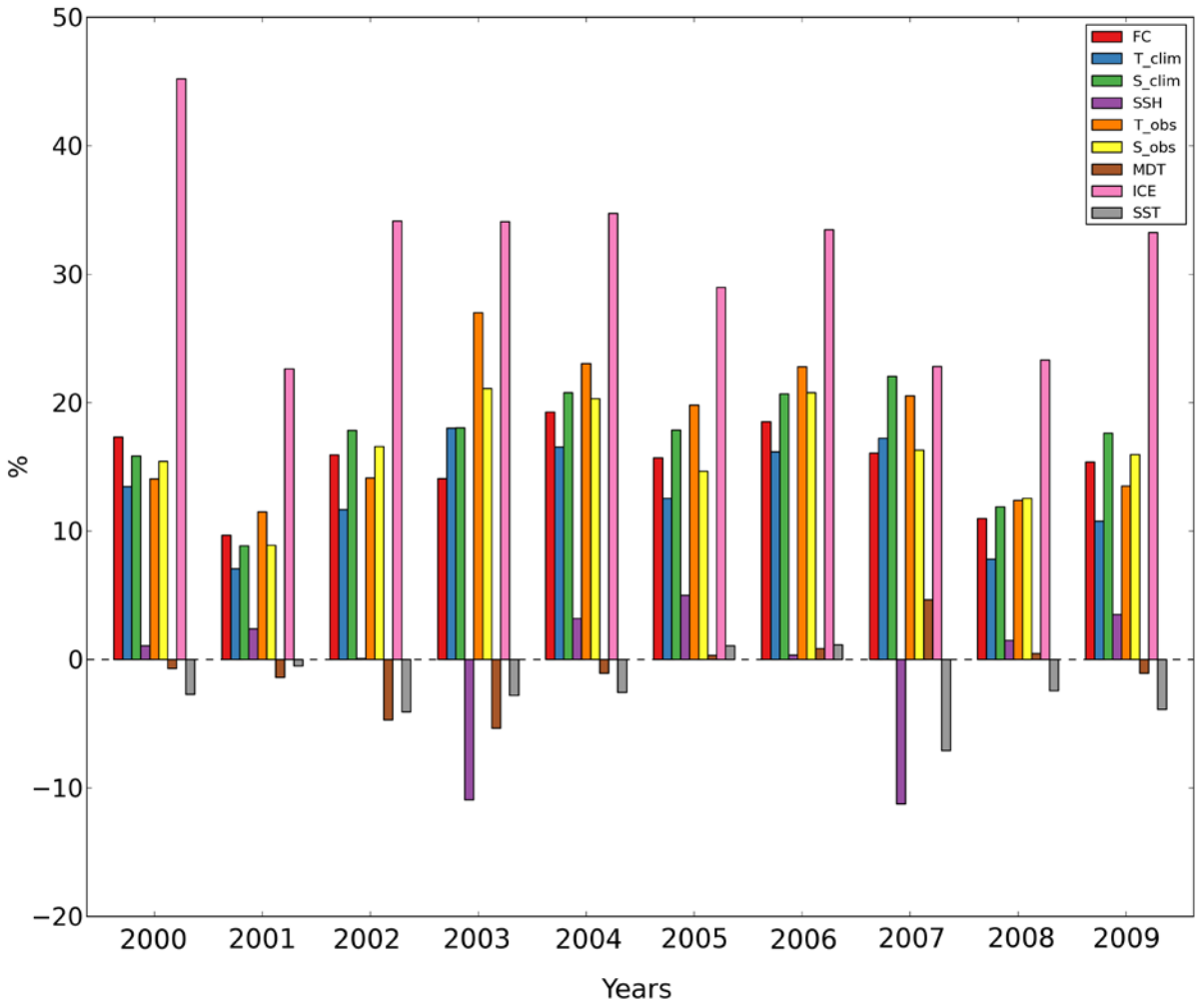

Fig. 5 Percentage of decrease in model/data difference .

Biggest total reduction (about 19%) obtained for the year 2004, while the smallest (about 10%) is obtained for the year 2001. Mean reduction for all years is about 15%. Biggest cost reduction in

individual variables obtained for the sea ice area, with overall mean of about 31% and maximum of about 45% reached in 2000.

Temperature and salinity obtained by *in sutu* measurements (T_obs and S_obs) also show good cost reduction, reaching maximum of 27% and 21% in 2003 (Fig. 6).

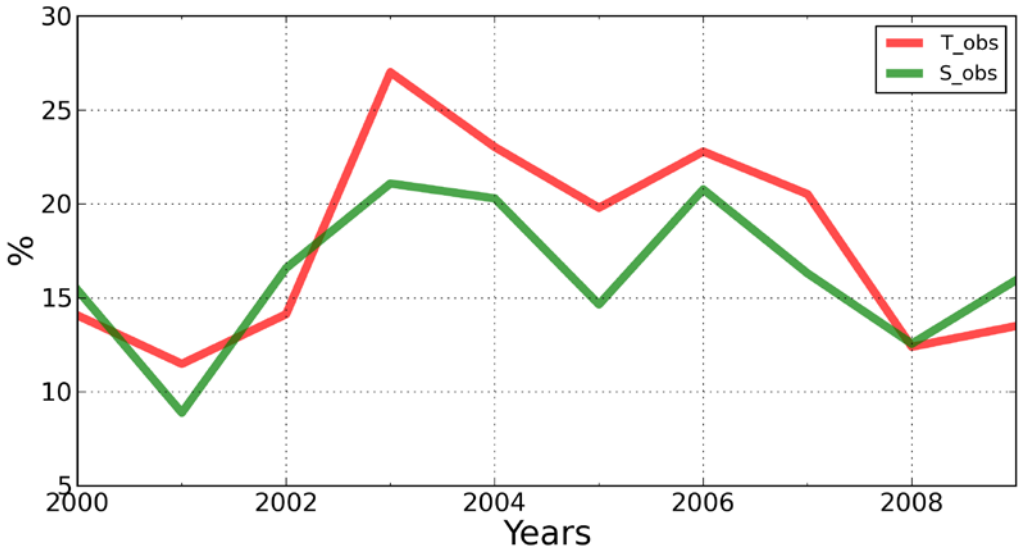

Fig. 6. Percentage of decrease in model/data difference for in situ measurements of temperature and salinity.

Least successful cost reduction obtained for SSH, mean dynamic topography (MDT) and sea surface temperature (SST). When misfit between model and observations for these variables decrease, it does not exceed few percent. However there are years wen model-data differences for some of this variables increase. Reasons for that are probably different for every individual variable, and have to be further investigated.

Overall reduction of the model-data difference is satisfactory. In the next sections we compare in detail some of the improved model characteristics with observations and show how they change compared to the initial guess.

5.1 Sea ice concentration.

Our system is among the first that use adjoint data assimilation to improve simulation of the sea ice. Fig. 7 shows example of improvement in sea ice concentration for winter time period (March of the year 2000). Most of the Arctic Ocean is covered by sea ice with high concentrations and biggest improvements are in the position of the ice edge. Most noticeable is decrease in sea ice concentration along the east coast of Greenland. During initial run of the model there is a tongue of sea ice extended towards the open ocean. After data assimilation the tongue did not disappeared completely, but it considerably shrinked.

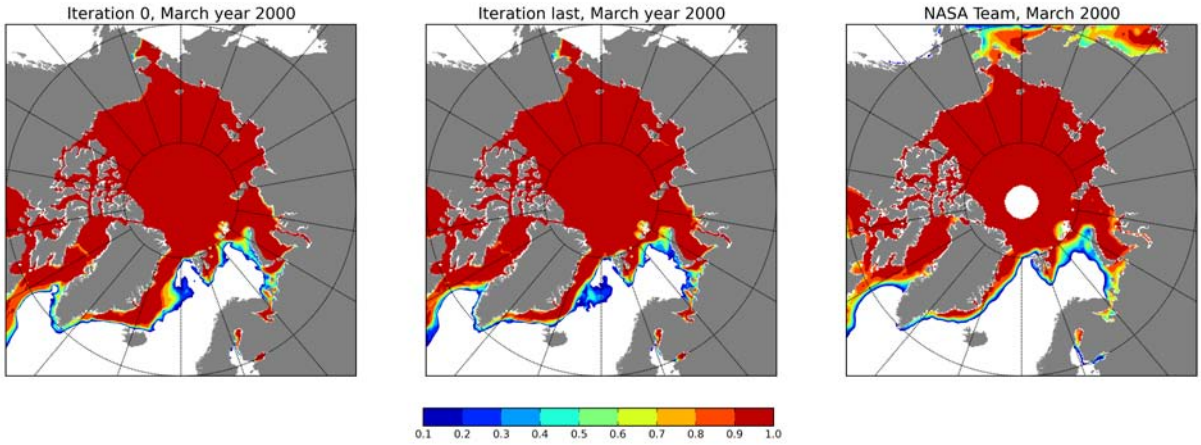

Fig. 7.Sea ice concentration for March 2000. First guess (left), last model iteration (middle), satellite observations.

During the summer period there are improvements both in sea ice edge and in sea ice concentration inside the sea ice field. Fig. 8 shows sea ice concentration for September 2000. Initially sea ice edge was not very far from observations, but after data assimilation it the match between model and data is almost exact. Area of low sea ice concentration to the north of the Laptev Sea disappears in the last iteration. There are also several relatively small scale features in the satellite observations that are reproduced after assimilation, for example one to the north of the New Siberian Islands.

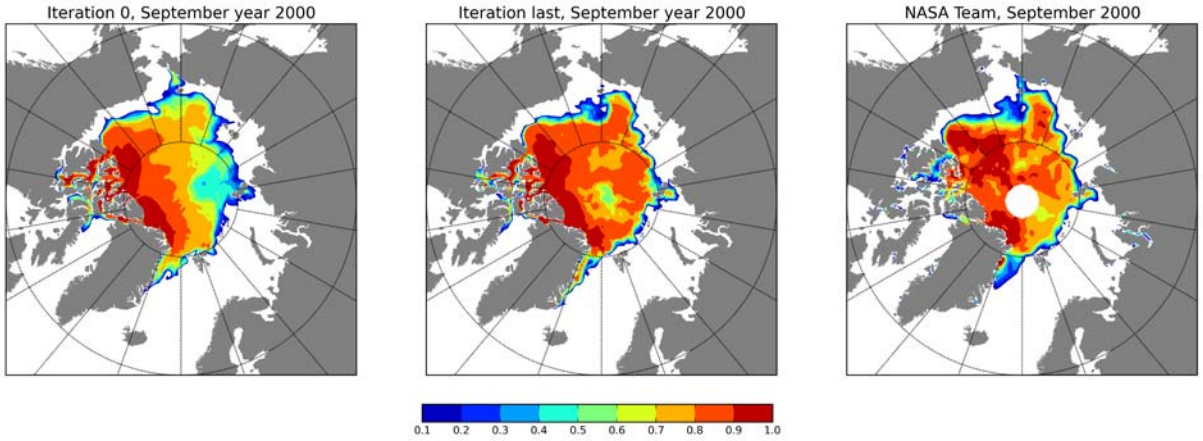

Fig.8. *Sea ice concentration for September 2000. First guess (left), last model iteration (middle), satellite observations.*

Satellites have no measurements around North Pole, and we provide no data to the model in this region. Unfortunately this lead to formation of the area with relatively low sea ice concentrations in the center of the Arctic Ocean. Although we have no satellite measurements there, field campains do not report any sea ice anomaly around the North Pole, so this feature is unrealistic in our simulations.

5.2 Temperature and salinity.

The assimilation of temperature and salinity profiles in the Arctic Ocean is challenging mainly because of the sparcity of the observations. We constrain the model by both available hydrological profiles and by the PHC climatology. In the framework of the MONARCH-A project it was shown (D2.4.1) that the ATL06 model is the base for our assimilation setup, overestimate temperature in the Eurasian Basin of the Arctic Ocean compared with climatology. However main data that have been used for climatology calculation are obtained mainly in 1970-1980. However recent observations (Dmitrenko et al 2008) show, that there is substantial increase in temperature during 2000s. Consequently climatology have reduced weight in assimilation, but high enough to provide a proper shape of vertical TS profile.

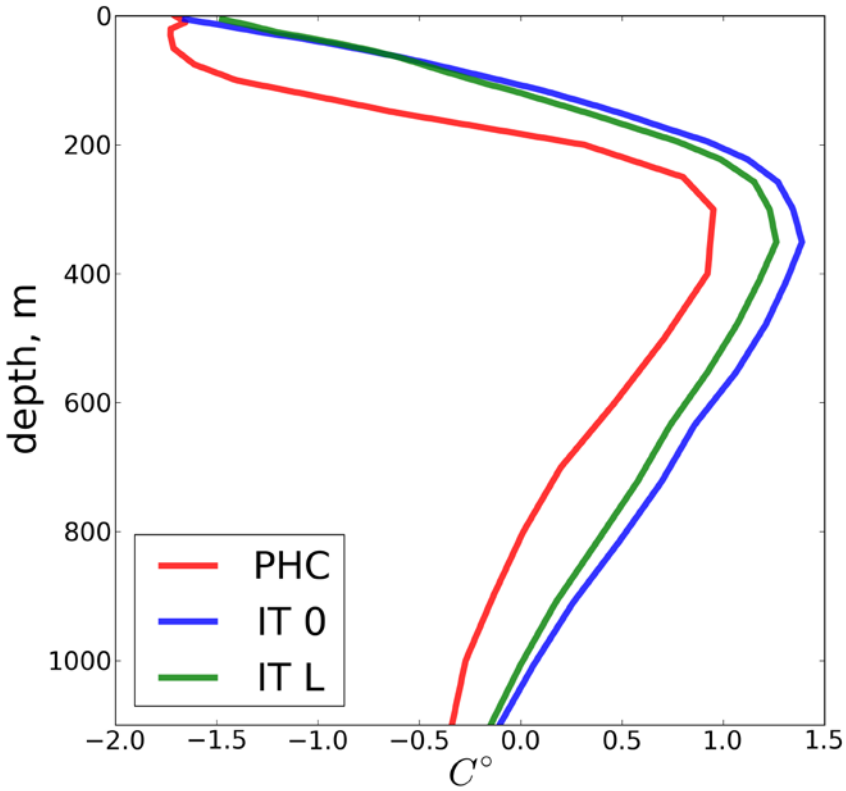

Fig.9. Mean vertical temperature profile in Eurasian Basin (150-1100 m). (red) PHC climatology, (blue) first guess, year 2003, (green) last iteration, year 2003.

Fig. 9 shows vertical temperature profile in Eurasian Basin of the Arctic Ocean for the year 2003 and for PHC climatology. Initial guess (blue) and last model iteration (green) are shown. In the Atlantic water layer data assimilation lead to cooling that makes model results closer to climatology. However representation of the temperature distribution in surface mixed layer in the model is still weak, despite data assimilation. This points to an underrepresentation of some physics that is responsible for formation of the mixed layer, and scarcity of the observational data in this region.

Distribution of salinity in the surface mixed layer also have the shape that is different from climatology (Fir.10), however the last iteration show more similarity with climatology, than the first guess.

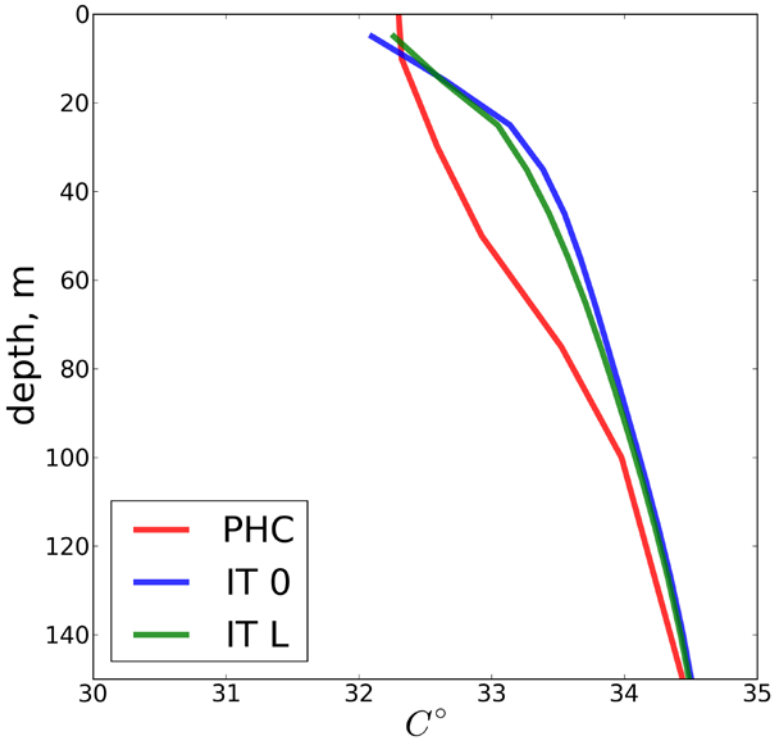

Fig.10. Mean vertical salinity profile (first 150 m) in Eurasian Basin. (red) PHC climatology, (blue) first guess, year 2003, (green) last iteration, year 2003.

Differences become smaller below 100 m (Fig. 11), were model simulation reproduce relatively steep pycnocline that extends down to about 300 meters. Then, at the depths close of the Atlantic Water core, salinity profile become vertical. Note that within this depth range data assimilation lead to salinity values that are closer to climatology.

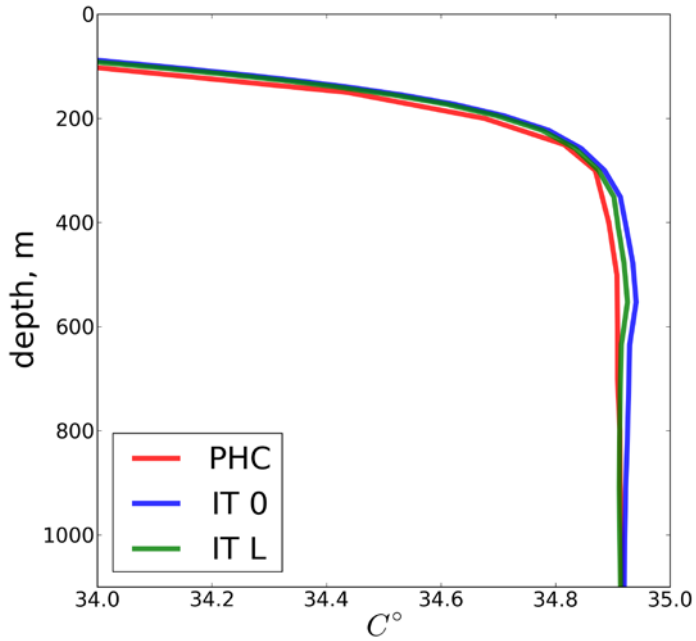

Fig.11. Mean vertical salinity profile (150-1100 m) in Eurasian Basin. (red) PHC climatology, (blue) first guess, year 2003, (green) last iteration, year 2003.

Properties in the deep parts of the Arctic Ocean defined to a large extend by the Atlantic water inflow. We look at the mean temperature and salinity differences between model runs with assimilation and without assimilation.

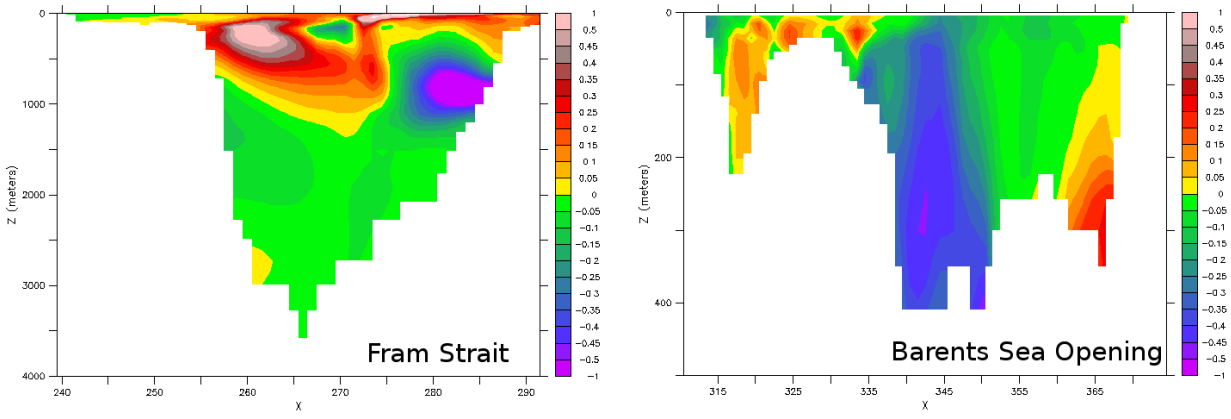

Fig. 12. Mean (2000-2009) temperature difference between model run with assimilation and without assimilation in the Fram Strait (left) and Barents sea Opening (right).

In the Fram Strait (Fig. 12, left) there is a significant decrease in temperature at about 1000 m depth on the eastern flank of the strait, witch is way below the core of Atlantic Water inflow in this region. There is also a strong increase in the sea surface temperature on the eastern part of the strait, and less pronounced increase in intermediate layers on the western flank of the strait, associated with East Greenland Current. In general there is an increase in temperature in the upper layers, and decrease in the deep layers of the strait.

In the Barents Sea opening (BSO) there is a decrease in temperatures of the main Atlantic water inflow and especially in the recirculation flow along the northern part of the side of the Bjørnøyrenna channel. Later indicate that after data assimilation there is more intensive cooling happening in the Barents Sea.

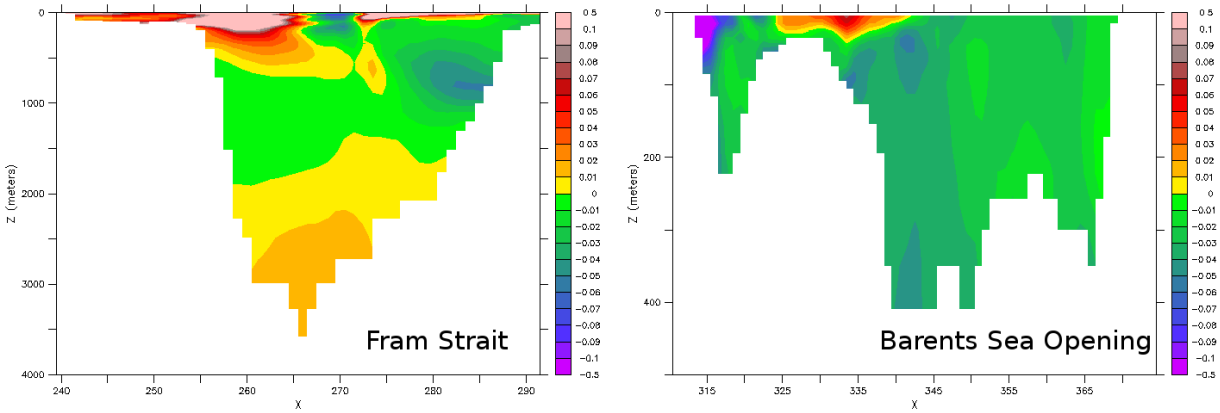

Fig. 13. Mean (2000-2009) salinity difference between model run with assimilation and without assimilation in the Fram Strait (left) and Barents Sea Opening (right).

Main patterns of difference in salinity in the Fram Strait (Fig. 13, left) are similar to those for the temperature. There is a strong decrease of salinity in the deeper layers of the western flank and strong increase in the upper layers over the western flank. Hence the water inflow to the Arctic Ocean through the Fram Strait becomes fresher, while water outflow become saltier.

Differences in salinity for the BSO are more homogeneous, in a way that for the most part of the water column there is a decrease in salinity. The only exception is the top layer over the northern flank of the Bjørnøyrenna channel, where salinity increased by up to 0.07 psu.

As shown on Fig. 9-11 in general water in the model is warmer and saltier compared to climatology, especially in the deep layers, so decrease in the temperature and freshening of the inflow can be considered as positive change. However for the core of the Atlantic water inflow in the Fram Strait

there is an increase in temperature. How this increase affects properties of the water masses in the Arctic Ocean should be further investigated.

5.3 Ocean circulation.

Due to sparseness and limited availability of direct current measurements in the Arctic Ocean, we still have limited understanding of Arctic Ocean circulation at intermediate depths and at the deep layers. Ocean surface currents are known better, since ice can be used to some extent as their proxy. We do not assimilate directly characteristics of the currents, but it is expected that they improve in the model as a consequence of assimilation of other parameters.

There are two large scale surface currents in the Arctic Ocean. Beaufort gyre – anticyclonic current with center close to the Beaufort Sea. It rotates water and ice in the Amerasian Basin of the Arctic Ocean. Transpolar Drift – current, that transports water and ice from East Siberian and Laptev seas, across the Arctic through the North Pole towards the Fram Strait.

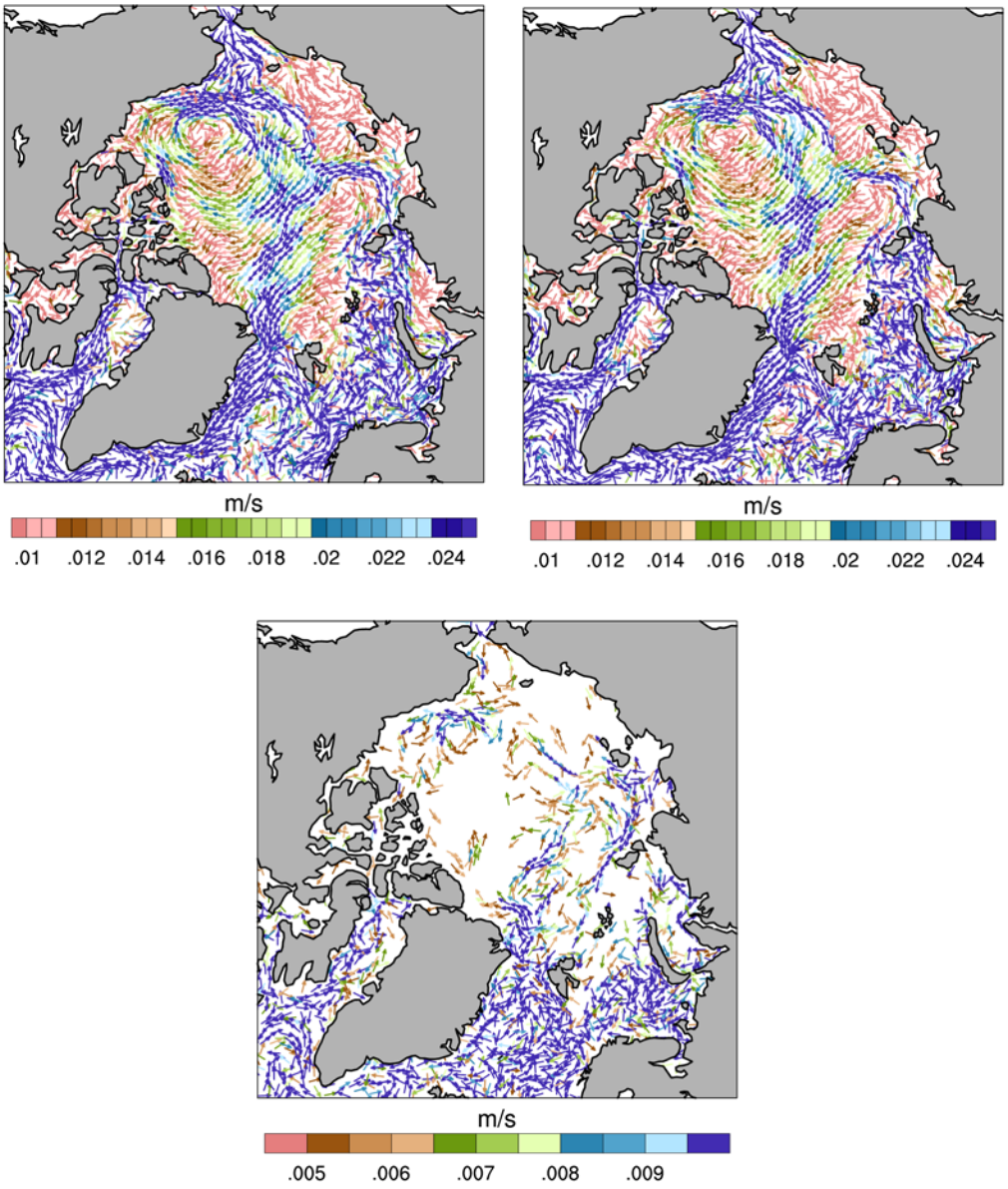

Fig. 14. Mean surface ocean currents for the period 2000-2009. (top left) First iterations, (top right) last iterations, (bottom) difference between last and first iterations.

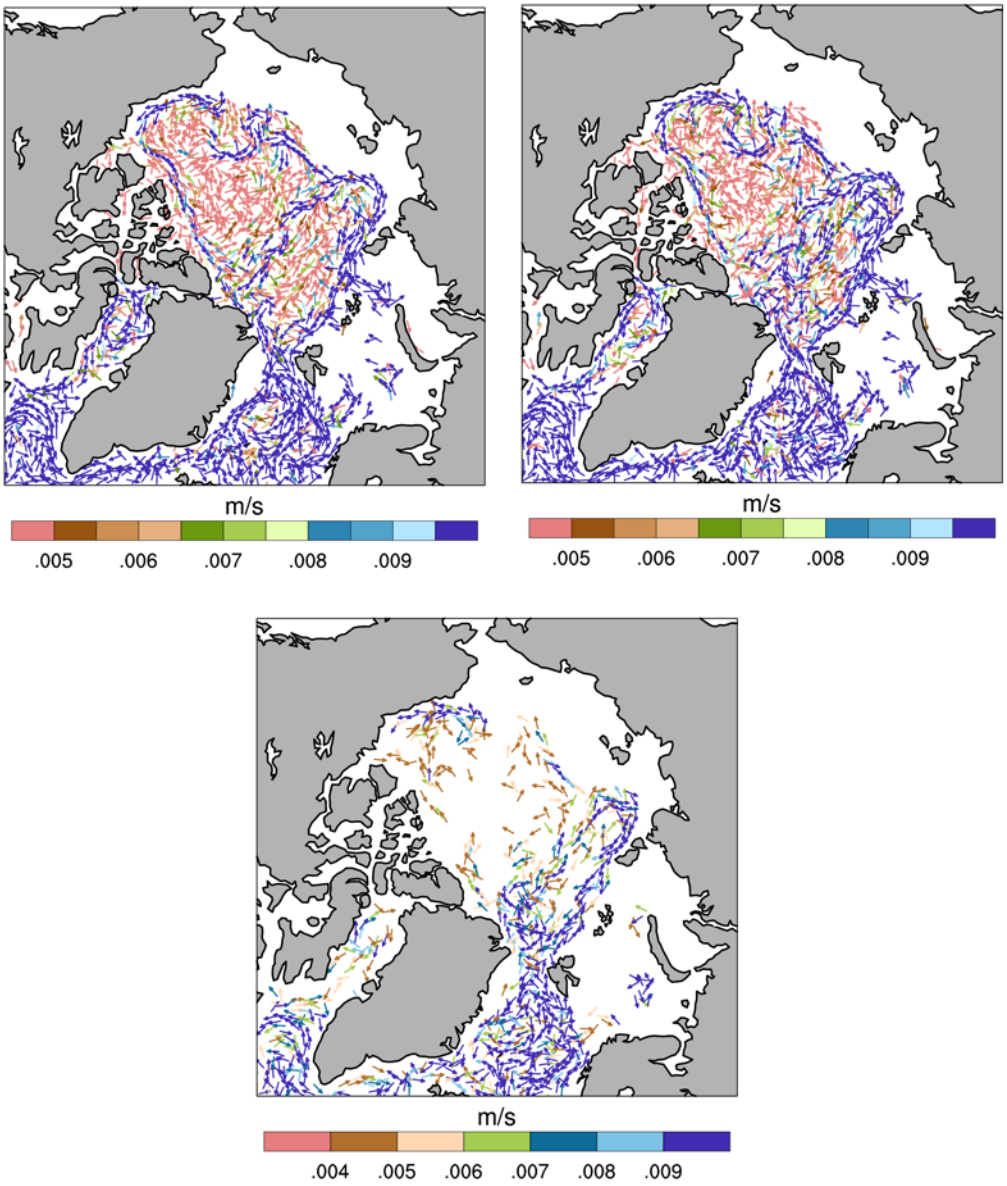

Fig. 15. Mean 300m ocean currents for the period 2000-2009. (top left) First iterations, (top right) last iterations, (bottom) difference between last and first iterations.

Fig. 14 show, that model reproduce both large-scale patterns of surface ocean circulations in the Arctic Ocean. Mean difference between first guess and last iterations indicate, that assimilation of the data lead to slow down of the surface circulation. In particular currents along Siberian shelf and

part of the Transdrift current that flows over the Lomonosov ridge become weaker. Another region, were currents become slower is to the north of Alaska.

The main feature of intermediate water circulation in the Arctic Ocean, that is mostly responsible for redistribution of relatively warm Atlantic water, is cyclonic movement of water along the shelf break. Proper simulation of this circulation for a long time was (and to some extend still is) a challenge for regional and global circulation models (Holloway et al 2007). Atlantic water enters the Arctic Ocean trough the Fram Strait and St. Anna Trough, and then distributed along the Siberian shelf towards Amerasian Basin. There is relatively well-known recirculation flow of Atlantic water over the Lomonosov Ridge.

Fig. 15 show, that model simulations were able to reproduce both along shelf break cyclonic circulation and recirculation along the Lomonosov ridge. General tendency is the same as in surface currents, the currents slow down. It is especially noticeable along the borders of the Barents, Kara and Laptev Seas. There is also one strong pattern that did not exist in the first iterations, but emerge after data assimilation – return flow along the Gakkel ridge.

5.4 Sea surface height

Even though some altimetric missions do have measurements relatively far north, the data obtained in the presence of sea ice were initially discarded. Later, with the development of new data processing techniques, it became possible to retrieve information about SSH in leads or over thin ice. From 4 years of ERS-2 measurements, Peacock and Laxon (2004) were the first to report SSH retrievals in ice-covered parts of the Arctic Ocean between 60◦ N and 81.5◦ N, and to compute an Arctic mean SSH. The first mean dynamic topography (MDT) of the Arctic Ocean was obtained by Forsberg et al. (2007) for the period 1995-2003 by subtracting the ArcGP geoid from combined ERS and ICESat altimetric measurements.

Since then MDT has been calculated by several groups. Kwok and Morison (2011) estimated it for 2004-2008 with the use of five winters of ICESat campaigns and the EGM2008 geoid (Pavlis et al. 2008). Giles et al. (2012) estimated the MDT over the period 1995-2010 using ERS-2 and Envisat data and the same geoid. More recently Farrell et al. (2012) calculated the MDT for 2003-2009 with the use of combined ICESat and Envisat data and the GOCO02S geoid (Goiginger et al. 2011), which in turn combines data derived from the Gravity Recovery And Climate Experiment (GRACE) (Tapley et al. 2003) and the Gravity field and steady-state Ocean Circulation Explorer (GOCE) (Pail et al. 2010), not using assimilation of altimetric measurements and therefore free of residual ocean signals.

For data assimilation we use MDT obtained by Danish Technical University in the framework of MONARCH-A project. While estimates of MDT from different groups vary in details, they all have several common features. The maximum elevation in the MDT is observed in the Beaufort Gyre, with

two distinct ”hills” along the northern coast of Greenland and in the East-Siberian and Laptev Seas. Most of the Eurasian basin is occupied by low values of MDT.

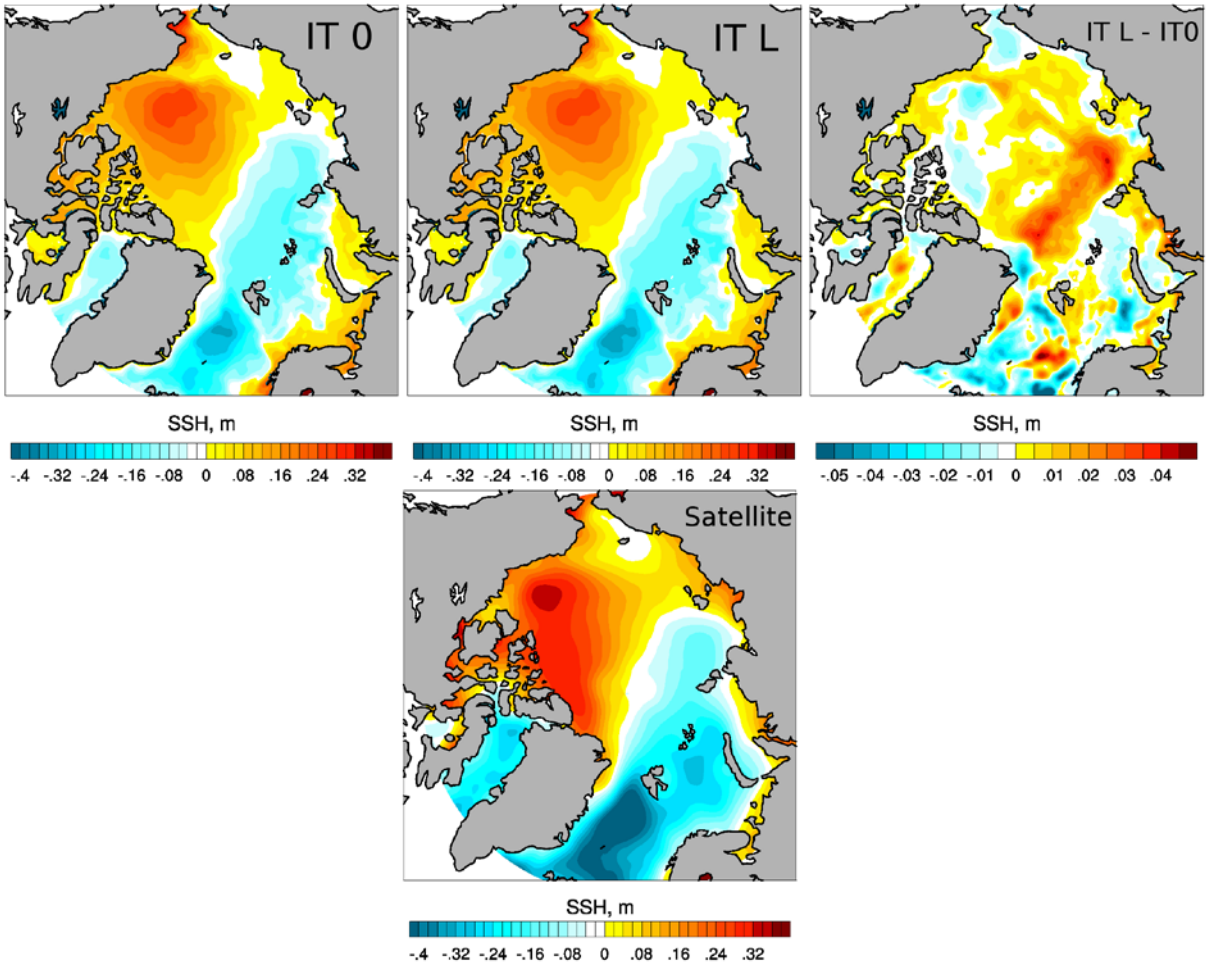

Fig. 16. Mean SSH anomalies to the north of 65 N for (top left) the first guess run, (top middle) last iteration, (top right) difference between first guess and last iteration, (bottom) based on satellite measurements.

As it can be seen from Fig. 5 overall reduction in model-data difference for mean SSH (MDT) did not exceed more than few percent, and for some years it is even increased. From the map of the spatial distribution of differences between initial guess and last iterations it is clear that most of the changes occur in the Eurasian Basin. This might be related to the overall freshening of this basin after data assimilation, as can be seen for the year 2003 (Fig. 11).

Comparison with mean satellite SSH anomaly (Fig. 16, bottom) show two main improvements in the model SSH field. First – the gradient between positive SSH anomalies in Amerasian basin and

negative SSH anomalies in Eurasian Basin is becoming less sharp, which make it closer to the spatiall distribution of satellite SSH. Second – there are stronger negative SSH values in the northern north Atlantic.

5.5 Volume, fresh water and heat transport

Arctic Ocean sometimes called Arctic Mediterranean, since it is semi-enclosed, and there are only few passages through which it can exchange heat and salt with Northern North Atlantic Ocean, and there is only one that allows exchange with Northern Pacific. In our setup the flow through the Bering Strait is prescribed, and we are not going to analyse it. Instead we will consider following straits: the Fram Strait, were warm salty Atlantic Water coming in to the Arctic along eastern flank of the strait and cold and fresher Arctic waters flow southward with the East Greenland Current. The Davis Strait integrates the entire outflow through Canadian Archipelago. The Barents Sea Opening (BSO) – another way for warm Atlantic waters to enter the Arctic. And the St. Anna Trough through which Atlantic Waters modified in the Barents Sea transported further to the Arctic Ocean.

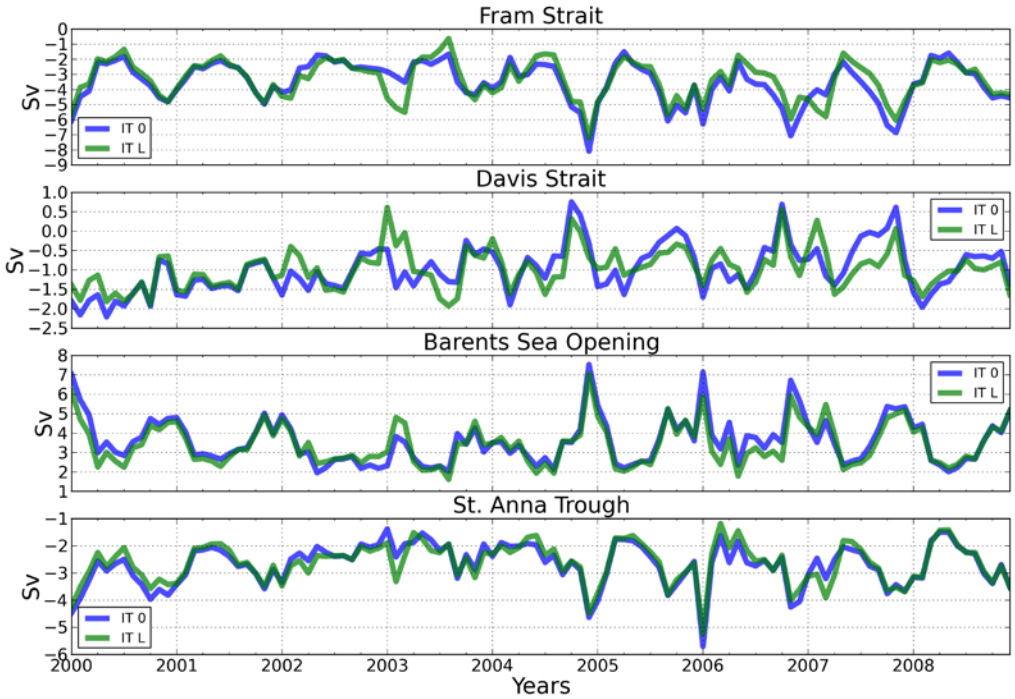

Fig.17. Volume transport through Arctic Ocean straits. (blue) – model before data assimilation, (green) – model after data assimilation.

Differences in volume transport between the runs with and without data assimilation (Fig. 17) overall are not large, but episodically can reach several Sv. Good example is the year 2003, when transport through the Fram Strait increased by about 2 Sv. Simultaneously there is also a large change in volume transport through BSO and Davis Strait. There is no defined pattern of change for any of the straits, so that for the differences can be both positive and negative.

The same is true for the heat transport (Fig. 18). Values for runs with and without data assimilation are quite close most of the time. Heat transport variability in the Fram Strait has much less of the seasonal signal compared to volume transport, especially in the first half of the record. On contrary in the Davis Strait there is more pronounced seasonal in heat transport than in the volume transport. Increase in volume transport during 2003 for run with data assimilation seems to be correlated with heat transport increase in the Fram Strait and St. Anna Trought, while for the other straits there is no significant difference in heat transport for this period.

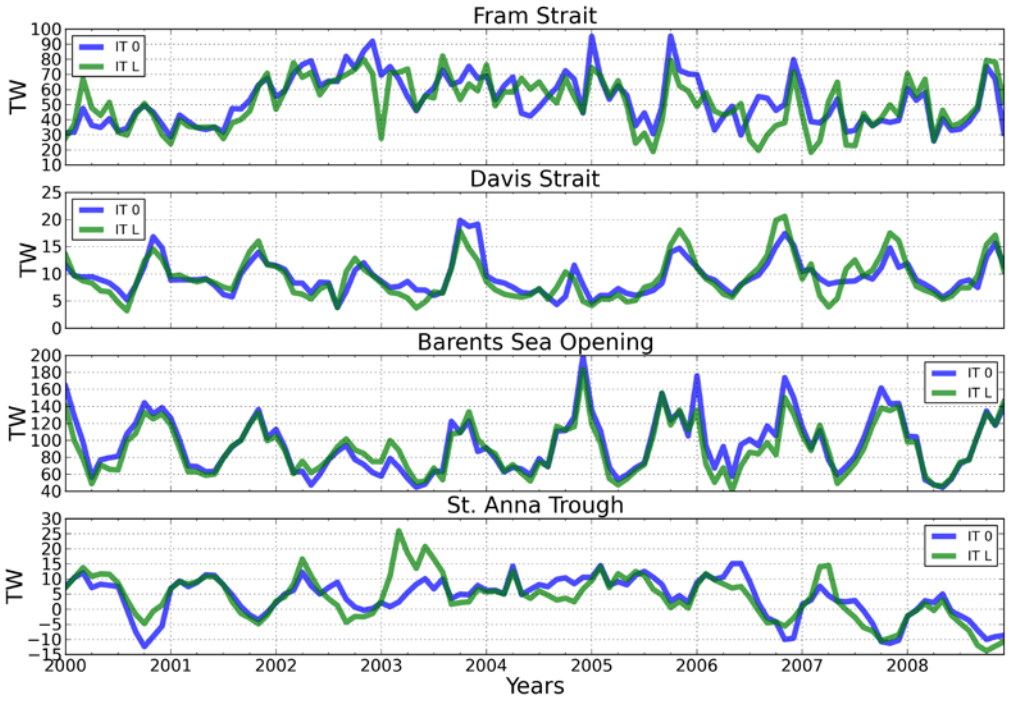

Fig.18. Heat transport through Arctic Ocean straits. (blue) – model before data assimilation, (green) – model after data assimilation.

When there is a strong seasonality in fresh water (FW) transport through Fram Strait and BSO, it is very hard to see seasonal signal in Davis Strait and St. Anna Trough. The largest differences between

runs with and without assimilation that reach about 60 mSv are in the Fram Strait during the year 2006. It might be associated with decrease in ice melting to the north of the Fram Strait during this period.

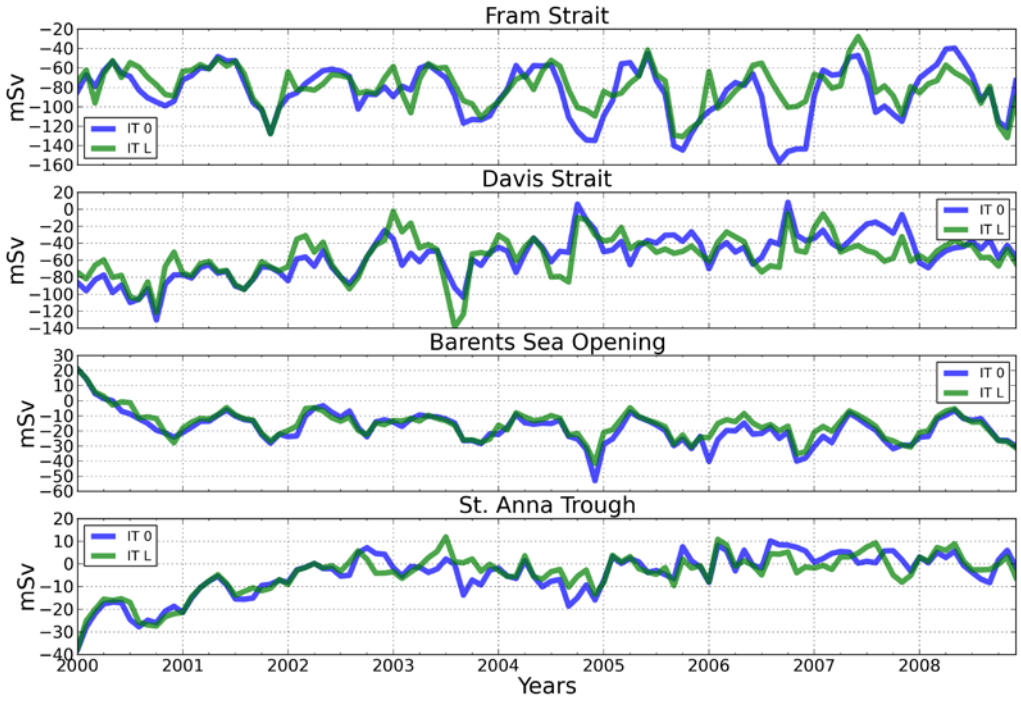

Fig.19. Fresh water (relative to 35psu) transport through Arctic Ocean straits. (blue) – model before data assimilation, (green) – model after data assimilation.

The mean values of different transports are summarized in the Table 2. There is generally a decrease in volume transport through all straits except for the Davis Strait, where small increase of 0.01 Sv is obtained. There is also decrease in heat transport through most of the straits, with BSO having the largest drop of about 4 TW. This indicate, that after data assimilation there is less heat coming to the Arctic from the North Atlantic, which makes mean temperature profile in the Arctic Ocean close to climatology. This is consistent with temperature differences that we obtained for transects across some of the straits (Fig. 12).

The biggest changes in fresh water transport obtained for the Fram Strait, with decrease of about 4 mSv. This indicate, that in run with assimilation water in the surface layer of the Arctic Ocean that is exported to the North Atlantic become saltier, and this can be clearly seen on Fig. 13. Decrease in

FW export through BSO is probably associated with freshening of the both inflow and recirculation current passing through this strait.

Table 2. Mean values of volume, heat and fresh water transport. The 0 sign is for run without data assimilation and L sign is for run with data assimilation. Blue color shows that there is a decrease, and red color shows that there is an increase in values between two runs.

	Volume 0 (Sv)	Volume L (Sv)	Heat 0 (TW)	Heat L (TW)	FW 0 (mSv)	FW L (mSv)
Fram Strait	**-3.50**	**-3.35**	**52.97**	**50.77**	**-84.81**	**-79.16**
Davis Strait	**-0.97**	**-0.98**	**9.44**	**9.28**	**-55.28**	**-55.38**
BSO	**3.60**	**3.44**	**95.17**	**90.72**	**-17.70**	**-15.60**
SAT	**-2.67**	**-2.62**	**3.94**	**3.98**	**-4.68**	**-4.27**

6 Summary

We have created a model setup, which is capable of data assimilating with use of adjoint technique. The model domain covers the Arctic Ocean and part of the North Atlantic that is an important source of heat and salt for the target region. Main assimilated parameters are: sea level, temperature and salinity profiles and sea ice concentration.

We completed a data assimilation experiment for the period of 2000-2009 that is characterized by substantial changes in the Arctic environment but also has relatively good data availability. On average we were able to reduce total model-data difference by 15 %. The largest mean reduction of 31% is obtained for the sea ice concentration. Reduction for temperature and salinity profiles is about 15-20% for different years.

The model shows good results for the sea ice assimilation. Originally too low concentrations in the central parts of the Arctic Ocean are increased, and sea ice edge during both winter and summer becomes very close to the observed one. However there is a yet unsolved problem of too low concentrations around the North Pole, where there is no satellite data to assimilate.

Comparison of mean temperature and salinity profiles to climatology show that after assimilation characteristics of the model become closer to climatological values. The main tendency is to push the model toward colder and fresher state in the Eurasian Basin that is achieved in part by decrease of temperature and salinity of water inflow to the Arctic Ocean through main straits.

The model reproduce all main patterns of surface ocean circulation, and data assimilation lead to partial slow down of the currents both on the surface and at the intermediate depth. This decrease in velocity is especially noticeable in the Eurasian Basin. At intermediate depth the return flow along Gakkel ridge emerge as a result of data assimilation.

Overall reduction in model-data difference for sea surface height is small. However spatial distribution shows some improvements. There is decrease in gradient between Eurasian and Amerasian Basins, and more realistic values in the North Atlantic.

Compared with run without assimilation there is generally decrease in volume, heat and fresh water transport through main passages of the Arctic Ocean, which is consistent with decrease in speed of the currents mentioned above. This changes lead to the model state that is closer to observations.

With the use of adjoint assimilation technique we produced a model simulation that is considerably closer to observations and in the same time dynamically consistent (reanalysis). This data can be used for further analysis of the reasons and consequences of changes in the Arctic Ocean. The

MONARCH-A aata assimilation system that was created during this project will be further used for reanalysis of the Arctic Ocean with possibly extended and improved data sets.

7 References

Madec, G., Imbard, M., 1996. A global ocean mesh to overcome the north pole singularity 12 (6), 381-388. URL http://dx.doi.org/10.1007/bf00211684

Kalnay, E., Kanamitsu, M., Kistler, R. and co-authors. 1996. The NCEP/NCAR 40-year reanalysis project. Bull. Am. Meteor. Soc. 77, 437–470.

Fekete, B., Vorosmarty, C. and Grabs, W. 1999. Global, composite runoff fields based on observed river discharge and simulated water balances, Global Runoff Data Center Tech. Rep. 22, Koblenz, Germany.

Large, W. G., J. C. Williams, and S. C. Doney, 1994: Ocean vertical mixing: A review and a model with a nonlocal boundary layer parameterization. Rev. Geophys., 32, 363–403.

Redi, M. H., 1982: Oceanic isopycnal mixing by coordinate rotation. J. Phys. Oceanogr., 12, 1154–1158.

Hibler WD (1979) Dynamic thermodynamic sea ice model. J Phys Oceanogr 9(4)

Hibler WD (1980) Modeling a variable thickness sea ice cover. Monthly Weather Review 108(12):1943, 19-73

Semtner AJ (1976) A model for the thermodynamic growth of sea ice in numerical investigations of climate. J Phys Oceanogr 6(3):379-389

Zhang J, Hibler WD, Steele M, Rothrock DA (1998) Arctic ice-ocean modeling with and without climate restoring. Journal of Physical Oceanography 28(2):191-217

Semtner AJ (1984) On modelling the seasonal thermodynamic cycle of sea ice in studies of climatic change. Climatic Change 6(1):27-37, DOI 10.1007/BF00141666

Hibler WD (1984) The role of sea ice dynamics in modeling CO2 increases. In: Hansen JE, Takahashi T (eds) Climate processes and climate sensitivity, Geophysical Monograph, vol 29, AGU, Washington, D.C., pp 238-253

Zhang J, Hibler WD (1997) On an efficient numerical method for modeling sea ice dynamics. Journal of Geophysical Research - Oceans 102(C4):null+, DOI 10.1029/96JC03744

Losch M, Menemenlis D, Campin JM, Heimbach P, Hill C (2010) On the formulation of sea-ice models. Part 1: Effects of different solver implementations and parameterizations. Ocean Modelling 33(1-2):129-144, DOI 10.1016/j.ocemod.2009.12.008

Nguyen AT, Menemenlis D, Kwok R (2011) Arctic ice-ocean simulation with optimized model pa- rameters: Approach and assessment. Journal of Geophysical Research 116(C4):C04,025+, DOI 10.1029/2010JC006573

Giering R, Kaminski T (1998) Recipes for adjoint code construction. ACM Trans Math Softw 24(4):437?474, DOI 10.1145/293686.293695

Giering R, Kaminski T, Slawig T (2005) Generating ef?cient derivative code with TAF adjoint and tangent linear Euler ?ow around an airfoil. Future Gener Comput Syst 21(8):1345?1355, DOI 10.1016/j.future.2004.11.003

Stammer D (2005) Adjusting internal model errors through ocean state estimation. J Phys Oceanogr 35(6):1143?1153, DOI 10.1175/JPO2733.1

Stammer D, Wunsch C, Giering R, Eckert C, Heimbach P, Marotzke J, Adcroft A, Hill CN, Marshall J (2002) Global ocean circulation during 1992-1997, estimated from ocean observations and a general circulation model. Journal of Geophysical Research (Oceans) 107(C9):1, DOI 10.1029/2001JC000888

Stammer D, Köhl A, Wunsch C (2007) Impact of accurate geoid fields on estimates of the ocean circulation. J Atmos Oceanic Technol 24(8):1464?1478, DOI 10.1175/JTECH2044.1

Stammer D, Park S, Köhl A, Lukas R, Santiago-Mandujano F (2008) Causes for large-scale hydrographic changes at the Hawaii ocean time series station. Journal of Physical Oceanography 38(9):1931?1948, DOI 10.1175/2008JPO3751.1

Köhl A, Stammer D (2004) Optimal observations for variational data assimilation. Journal of Physical Oceanography 34(3):529?542, DOI 10.1175/2513.1

Köhl A, Stammer D (2008) Variability of the meridional overturning in the North Atlantic from the 50-year GECCO state estimation. Journal of Physical Oceanography 38(9):1913?1930, DOI 10.1175/2008JPO3775.1

Fenty I, Heimbach P (2012a) Coupled sea Ice-Ocean state estimation in the labrador sea and Baffn bay. J Phys Oceanogr DOI 10.1175/JPO-D-12-065.1

Fenty I, Heimbach P (2012b) Hydrographic preconditioning for seasonal sea ice anomalies in the labrador sea. J Phys Oceanogr DOI 10.1175/JPO-D-12-064.1

Steele M, Morley R, Ermold W (2001) PHC: A global ocean hydrography with a high-quality Arctic Ocean. J Clim 14(9):2079-2087

Nilsen J. Even Ø., Hjálmar Hátún , Kjell Arne Mork , Héðinn Valdimarsson (2008) The NISE Dataset. Faroese Fisheries Laboratory Technical Report 08-01.

Curry, R., 2001, HydroBase 2 - A database of hydrographic profiles and tools for climatological analysis. Technical reference.

Cavalieri, D., C. Parkinson, P. Gloersen, and H. J. Zwally. 1996, updated yearly. Sea Ice Concentrations from Nimbus-7 SMMR and DMSP SSM/I-SSMIS Passive Microwave Data. 2000-2009. Boulder, Colorado USA: National Snow and Ice Data Center.

Dmitrenko, I. A., et al., 2008: Toward a warmer Arctic Ocean: Spreading of the early 21th century Atlantic Water warm anomaly along the Eurasian Basin margins. Journal of Geophysical Research, 113, C05 023+, doi:10.1029/2007JC004158.

Holloway, G., Dupont, F., Golubeva, E., Häkkinen, S., Hunke, E., Jin, M., Karcher, M., Kauker, F., Maltrud, M., Maqueda, M. A. M., Maslowski, W., Platov, G., Stark, D., Steele, M., Suzuki, T., Wang, J., Zhang, J., Mar. 2007. Water properties and circulation in arctic ocean models. Journal of Geophysical Research 112 (C4), C04S03+.

Peacock, N. R. and S. W. Laxon, 2004: Sea surface height determination in the Arctic Ocean from ERS altimetry. Journal of Geophysical Research, 109 (C7), C07 001+, doi:10.1029/2001JC001026.

Forsberg, R., et al., 2007: Combination of Spaceborne, Airborne and In-Situ Gravity Measurements in Support of Arctic Sea Ice Thickness Mapping. Tech. Rep. 7, Danish National Space Center.

Kwok, R. and J. Morison, 2011: Dynamic topography of the ice-covered Arctic Ocean from ICESat. Geophysical Research Letters, 38 (2), L02 501+, doi:10.1029/2010GL046063.

Pavlis, N. K., S. A. Holmes, S. C. Kenyon, and J. K. Factor, 2008: An Earth Gravitational Model to Degree 2160:EGM2008. presented at the 2008 General Assembly of the European Geosciences Union, Vienna, Austria, April 13-18.

Giles, K. A., S. W. Laxon, A. L. Ridout, D. J. Wingham, and S. Bacon, 2012: Western Arctic Ocean freshwater storage increased by wind-driven spin-up of the Beaufort Gyre. Nature Geosci, advance online publication (3), 194–197, doi:10.1038/ngeo1379.

Farrell, S. L., D. C. McAdoo, S. W. Laxon, H. J. Zwally, D. Yi, A. Ridout, and K. Giles, 2012: Mean dynamic topography of the Arctic Ocean. Geophysical Research Letters, 39 (1), L01 601+, doi:10.1029/2011GL050052.

Goiginger, H., et al., 2011: The combined satellite-only global gravity field model GOCO02S. In EGU General Assembly 2011, vol ume 13.

Tapley, B. D., D. P. Chambers, S. Bettadpur, and J. C. Ries, 2003: Large scale ocean circulation from the GRACE GGM01 Geoid. Geophysical Research Letters, 30 (22), 2163+, doi:10.1029/2003GL018622.

Pail, R., et al., 2010: Combined satellite gravity field model GOCO01S derived from GOCE and GRACE. Geophysical Research Letters, 37 (20), L20 314+, doi:10.1029/ 2010GL044906.

END OF DOCUMENT